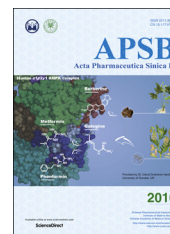




Chinese Pharmaceutical Association  
Institute of Materia Medica, Chinese Academy of Medical Sciences

Acta Pharmaceutica Sinica B

[www.elsevier.com/locate/apsb](http://www.elsevier.com/locate/apsb)  
[www.sciencedirect.com](http://www.sciencedirect.com)



ORIGINAL ARTICLE

# Sesquiterpene glycosides from the roots of *Codonopsis pilosula*



Yueping Jiang<sup>a,b</sup>, Yufeng Liu<sup>a</sup>, Qinglan Guo<sup>a</sup>, Chengbo Xu<sup>a</sup>,  
Chenggen Zhu<sup>a</sup>, Jiangong Shi<sup>a,\*</sup>

<sup>a</sup>State Key Laboratory of Bioactive Substance and Function of Natural Medicines, Institute of Materia Medica, Chinese Academy of Medical Sciences and Peking Union Medical College, Beijing 100050, China

<sup>b</sup>Department of Pharmacy, Xiangya Hospital, Central South University, Changsha 410008, China

Received 6 August 2015; received in revised form 10 September 2015; accepted 14 September 2015

## KEYWORDS

*Codonopsis pilosula*;  
Campanulaceae;  
Sesquiterpene glycoside;  
Codonopsesquilosides  
A–C;  
C<sub>15</sub> carotenoid;  
Gymnomitrane;  
Eudesmane

**Abstract** Three new sesquiterpene glycosides, named codonopsesquilosides A–C (**1–3**), were isolated from an aqueous extract of the dried roots of *Codonopsis pilosula*. Their structures including absolute configurations were determined by spectroscopic and chemical methods. These glycosides are categorized as C<sub>15</sub> carotenoid (**1**), gymnomitrane (**2**), and eudesmane (**3**) types of sesquiterpenoids, respectively. Compound **1** is the first diglycoside of C<sub>15</sub> carotenoids to be reported. Compound **2** represents the second reported example of gymnomitrane-type sesquiterpenoids from higher plants. The absolute configurations were supported by comparison of the experimental circular dichroism (CD) spectra with the calculated electronic CD (ECD) spectra of **1–3**, their aglycones, and model compounds based on quantum-mechanical time-dependent density functional theory. The influences of the glycosyls on the calculated ECD spectra of the glycosidic sesquiterpenoids, as well as some nomenclature and descriptive problems with gymnomitrane-type sesquiterpenoids are discussed.

© 2016 Chinese Pharmaceutical Association and Institute of Materia Medica, Chinese Academy of Medical Sciences. Production and hosting by Elsevier B.V. This is an open access article under the CC BY-NC-ND license (<http://creativecommons.org/licenses/by-nc-nd/4.0/>).

\*Corresponding author. Tel.: +86 10 83154789; fax: +86 10 63037757.

E-mail address: [shijg@imm.ac.cn](mailto:shijg@imm.ac.cn) (Jiangong Shi).

Peer review under responsibility of Institute of Materia Medica, Chinese Academy of Medical Sciences and Chinese Pharmaceutical Association.

## 1. Introduction

The dried roots of *Codonopsis pilosula* (Franch.) Nannf. (Campanulaceae), known as “dang shen” in Chinese, are one of the most common drugs in traditional Chinese medicine and normally are used as a substitute for the much more costly *Panax ginseng* as tonic agents exhibiting similar therapeutic effects<sup>1</sup>. Although some chemical constituents and pharmacological activities have been reported, previous work was mainly carried out on ethanol or methanol extracts of this natural product<sup>2</sup>, which is not consistent with practical utilization of herbal medicines including various formulations containing “dang shen” by decocting with water. As part of a program to systematically study the chemical diversity of traditional Chinese medicines and their biological effects, focusing on water-soluble and minor constituents<sup>3–14</sup>, an aqueous decoction of “dang shen” was investigated. Previously, we reported twelve new constituents from the decoction<sup>2,15</sup>, including an unsaturated  $\omega$ -hydroxy fatty acid, 4 acetylenes, and 7 C<sub>14</sub>-polyacetylene glucosides, along with preliminary bioassays. Continuation of our investigation on the same extract led to characterization of three new minor sesquiterpene glycosides named codonopsesquiosides A–C (**1–3**) (Fig. 1). Herein, reported are details of the isolation and structural elucidation of the new isolates.

## 2. Results and discussion

Compound **1**, a white amorphous powder with  $[\alpha]_D^{20} +26.3$  (*c* 0.04, MeOH), showed IR absorption bands for hydroxyl (3395 cm<sup>-1</sup>), double bond (3010 cm<sup>-1</sup>), and conjugated carbonyl (1645 cm<sup>-1</sup>) functional groups. The molecular formula of **1**, C<sub>26</sub>H<sub>40</sub>O<sub>11</sub>, was indicated by HR-ESI-MS at *m/z* 551.2461 [M+Na]<sup>+</sup> (Calcd. for C<sub>26</sub>H<sub>40</sub>O<sub>11</sub>Na, 551.2463) and NMR spectroscopic data (Table 1). The <sup>1</sup>H NMR spectrum of **1** in DMSO-*d*<sub>6</sub> showed signals attributable to a *trans*-disubstituted double bond at  $\delta_H$  6.23 (d, *J*=15.6 Hz, H-8) and 5.61 (dd, *J*=15.6 and 9.6 Hz, H-7); two trisubstituted double bonds at  $\delta_H$  5.80 (s, H-4) and 5.60 (d, *J*=7.2 and 6.6 Hz, H-10); an oxygen-bearing methylene at  $\delta_H$  4.32 (dd, *J*=12.6 and 6.6, H-11a) and 4.19 (dd, *J*=12.6 and 7.2 Hz, H-11b); an aliphatic methine at  $\delta_H$  2.67 (dd, *J*=9.6, H-6); an isolated aliphatic methylene at  $\delta_H$  2.41 (d, *J*=16.8 Hz, H-2a) and 1.97 (d, *J*=16.8 Hz, H-2b); and four tertiary methyl groups at  $\delta_H$  1.84 (s, H<sub>3</sub>-13), 1.73 (s, H<sub>3</sub>-12), 0.95 (s, H<sub>3</sub>-14), and 0.88 (s, H<sub>3</sub>-15). Additionally, the spectrum showed characteristic signals for two glycosyl units (Table 1) with anomeric protons at  $\delta_H$  4.13 (d, *J*=7.8 Hz, H-1') and 4.86 (d, *J*=3.0 Hz, H-1''), respectively. The <sup>13</sup>C NMR and distortionless enhanced polarization transfer (DEPT) spectra of **1** showed 26 carbon resonances (Table 1) corresponding the above units, a carbonyl ( $\delta_C$  197.9, C-3), and a

quaternary carbon ( $\delta_C$  35.9, C-1). These spectroscopic data indicates that **1** is a monocyclic sesquiterpene diglycoside for which the structure was further elucidated by 2D NMR data analysis.

The proton and proton-bearing carbon signals in the NMR spectra were assigned by cross-peaks in the <sup>1</sup>H–<sup>1</sup>H COSY and HSQC spectra. The heteronuclear multiple bond correlation (HMBC) correlations from H<sub>2</sub>-2 to C-1, C-3, C-6, C-14, and C-15; from H-4 to C-3, C-6, and C-13; from H-6 to C-1, C-2, C-4, C-5, C-13, C-14 and C-15; from H<sub>3</sub>-13 to C-4, C-5, and C-6; and from both H<sub>3</sub>-14 and H<sub>3</sub>-15 to C-1, C-2, and C-6 (Fig. 2); together with their chemical shifts, revealed the presence of a 6-substituted 1,1,5-trimethylhex-4-en-3-one moiety in **1**. The <sup>1</sup>H–<sup>1</sup>H COSY correlations of H-6/H-7/H-8 and H-10/H-11 and the HMBC correlations from H-6 to C-7 and C-8; from H-8 to C-6, C-9, C-10, and C-12; from H-10 to C-8 and C-12; from H<sub>2</sub>-11 to C-9 and C-10; and from H<sub>3</sub>-12 to C-8, C-9, and C-10 demonstrated that there was an 11-oxygen substituted 9-methylpenta-7,9-dien-7-yl side chain at C-6 of the hex-4-en-3-one moiety. In addition, the <sup>1</sup>H–<sup>1</sup>H COSY correlations of H-1'/H-2'/H-3'/H-4'/H-5'/H-6' and their vicinal coupling constants, combined with the HMBC correlations from H<sub>2</sub>-11 to C-1' and from H-1' to C-11, indicated the occurrence of a  $\beta$ -glucopyranosyloxy at C-11. The <sup>1</sup>H–<sup>1</sup>H COSY cross-peaks H-1''/H-2'' and the HMBC correlations from H-1'' to C-4'' and C-6', from H<sub>2</sub>-6' to C-1'', from both H<sub>2</sub>-4'' and H<sub>2</sub>-5'' to C-3'', in combination with the quaternary nature of C-3'', suggested that there was a  $\beta$ -apiofuranosyloxy at C-6' of the  $\beta$ -glucopyranosyl. This was supported by NMR data comparison of the diglycosyl in **1** with those previously reported for structurally related compounds<sup>16,17</sup> and further confirmed by enzymatic hydrolysis of **1** with snailase. From the hydrolysate of **1**, a sugar mixture of glucose and apiose was isolated by column chromatography over silica gel (CH<sub>3</sub>CN–H<sub>2</sub>O, 8:1, *v/v*) and identified by thin-layer liquid chromatography (TLC) comparison with authentic sugar samples. The sugar mixture and authentic D- and L-glucose and D- and L-apiose were separately allowed to react with L-cysteine methyl ester and arylisothiocyanate<sup>18</sup>. Subsequent HPLC analysis indicated that two sugar derivatives from the mixture had retention time (*t*<sub>R</sub>) identical to those of D-glucose and D-apiose derivatives. This verified that both glycosyl units in **1** possessed the D-configuration. Similarity of the NMR data and the circular dichroism (CD) spectra between **1** and the reported acetylated  $\beta$ -D-glucopyranoside<sup>19</sup> indicated that these two compounds have the same aglycone moiety including geometric and absolute configurations. The configuration was further supported by comparison of the experimental CD spectrum of **1** with the calculated electronic CD (ECD) spectra of **1**, its aglycone, and a model compound with substitution of the diglycosyl unit by a methyl group (Fig. 3) predicted from the quantum-mechanical, time-dependent density functional theory (TDDFT) calculations<sup>20</sup>. Therefore, the structure of compound **1** was determined and named codonopsesquioside A. This compound can also be named (*R*)-dehydroxyabscisic alcohol  $\beta$ -D-apiofuranosyl-(1'' $\rightarrow$ 6')- $\beta$ -D-glucopyranoside since the aglycone differs from (*S*)-abscisic alcohol only in the absence of hydroxyl group at the chiral center<sup>21</sup>.

Compound **2**, a white amorphous powder with  $[\alpha]_D^{20} -46.7$  (*c* 0.04, MeOH), has the molecular formula C<sub>26</sub>H<sub>40</sub>O<sub>11</sub> as indicated by HR-ESI-MS at *m/z* 529.2637 [M+H]<sup>+</sup> (Calcd. for C<sub>26</sub>H<sub>41</sub>O<sub>11</sub>, 529.2643) and 551.2462 [M+Na]<sup>+</sup> (Calcd. for C<sub>26</sub>H<sub>40</sub>O<sub>11</sub>Na, 551.2463). The IR spectrum of **2** showed the presence of hydroxyl (3395 cm<sup>-1</sup>) and conjugated carbonyl (1747 and 1647 cm<sup>-1</sup>) groups. The NMR spectra of **2** (Table 1) displayed the resonances

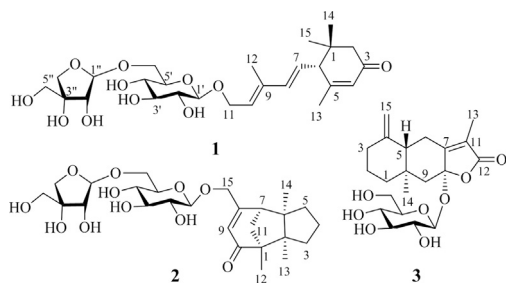


Figure 1 The structures of compounds **1–3**.

**Table 1**  $^1\text{H}$  and  $^{13}\text{C}$  NMR spectral data ( $\delta$ ) for compounds **1**–**3**.<sup>a</sup>

No.	<b>1</b>		<b>2</b>		<b>3</b> <sup>b</sup>	
	$\delta_{\text{H}}$	$\delta_{\text{C}}$	$\delta_{\text{H}}$	$\delta_{\text{C}}$	$\delta_{\text{H}}$	$\delta_{\text{C}}$
1a		35.9		61.4	1.51 m	41.8
1b					1.30 ddd (10.5, 6.0, 4.5)	
2a	2.41 d (16.8)	47.3		56.3	1.61 m	23.2
2b	1.97 d (16.8)					
3a		197.9	1.38 dd (12.0, 6.0)	38.8	2.32 ddd (13.2, 3.0, 1.8)	36.7
3b			1.12 m		1.98 ddd (13.2, 7.2, 6.0)	
4a	5.80 s	124.8	1.48 m	27.6		149.9
4b			1.37 m			
5a		162.0	1.64 ddd (12.0, 6.0, 3.6)	40.0	1.91 dd (12.6, 1.2)	52.0
5b			1.34 dd (12.0, 6.0)			
6a	2.67 d (9.6)	55.2		57.9	2.76 ddd (13.2, 12.6, 1.2)	26.3
6b					2.66 dd (13.2, 3.0)	
7	5.61 dd (15.6, 9.6)	126.5	2.19 d (4.8)	50.3		162.3
8	6.23 d (15.6)	137.2		170.6		105.3
9a		135.9	6.08 d (0.6)	123.8	2.27 d (13.2)	51.7
9b					1.49 d (13.2)	
10	5.60 dd (7.2, 6.6)	127.3		208.3		37.4
11a	4.32 dd (12.6, 6.6)	64.4	2.03 dd (12.0, 4.8)	47.9		123.1
11b	4.19 dd (12.6, 7.2)		1.82 d (12.0)			
12	1.73 s	12.6	0.98 s	17.9		171.9
13	1.84 s	23.0	0.96 s	23.0	1.78 d (0.6)	8.2
14	0.95 s	27.4	1.15 s	28.3	1.00 s	17.3
15a	0.88 s	26.8	4.42 dd (17.4, 1.8)	72.2	4.81 d (1.2)	107.0
15b			4.33 dd (17.4, 1.8)		4.63 d (1.2)	
1'	4.13 d (7.8)	101.8	4.26 d (7.8)	104.5	4.15 d (7.8)	97.3
2'	2.95 t (7.8)	73.3	3.29 t (7.8)	78.0	3.23 ddd (9.0, 7.8, 3.0)	74.3
3'	3.23 dd (9.0, 7.8)	76.6	3.19 t (7.8)	75.0	3.36 t (9.0)	77.9
4'	2.97 t (9.0)	70.3	3.24 m	71.5	3.30 ddd (9.6, 6.0, 3.0)	71.7
5'	3.11 t (9.0)	75.6	3.34 m	78.0	3.12 m	78.2
6'a	3.83 d (11.4)	67.7	3.90 dd (11.4, 1.8)	68.5	3.80 ddd (11.4, 4.8, 3.0)	62.8
6'b	3.40 dd (11.4, 7.2)		3.55 dd (11.4, 6.0)		3.58 ddd (11.4, 6.6, 6.0)	
1''	4.86 d (3.0)	109.3	4.93 d (2.4)	111.0		
2''	3.74 (1.8)	75.9	3.84 d (2.4)	78.0		
3''		78.8		80.5		
4''a	3.84 d (9.0)	73.2	3.89 d (9.6)	75.0		
4''b	3.57 d (9.0)		3.69 d (9.6)			
5''	3.31 m	63.1	3.52 s	65.6		

<sup>a</sup>NMR data ( $\delta$ ) were measured at 600 MHz for  $^1\text{H}$  NMR and 150 MHz for  $^{13}\text{C}$  NMR in DMSO- $d_6$  for **1**, in MeOH- $d_4$  for **2**, and in acetone- $d_6$  for **3**, respectively. Proton coupling constants ( $J$ ) in Hz are given in parentheses. The assignments were based on  $^1\text{H}$ - $^1\text{H}$  COSY, HSQC, and HMBC experiments.

<sup>b</sup> $^1\text{H}$  NMR data for hydroxyl protons of **3**:  $\delta_{\text{H}}$  4.23 (1H, brs, OH-4'), 4.21 (1H, d,  $J=3.0$  Hz, OH-2'), 4.12 (1H, d,  $J=3.0$  Hz, OH-3'), 3.40 (1H, t,  $J=6.6$  Hz, OH-6').

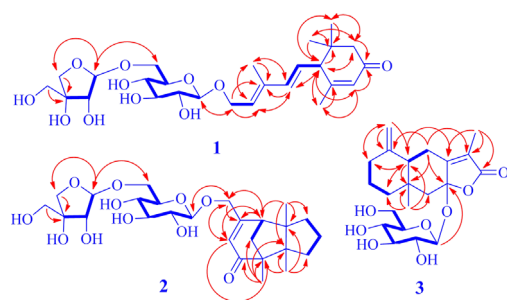


**Figure 2** The  $^1\text{H}$ - $^1\text{H}$  COSY (thick line) and key HMBC (arrows, from  $^1\text{H}$  NMR to  $^{13}\text{C}$  NMR) correlations of compounds **1**–**3**.

attributable to three tertiary methyls, five methylenes (an oxygen-bearing), one methine, a trisubstituted double bond, and four quaternary carbons including a carbonyl carbon ( $\delta_{\text{C}}$  208.3, C-10), as well as the signals ascribable to the same diglycosyl moiety as that of **1**. These spectroscopic data indicates that **2** is a tricyclic sesquiterpene  $\beta$ -D-apiofuranosyl-(1''  $\rightarrow$  6')- $\beta$ -D-glucopyranoside, with an aglycone moiety different from that of **1**. In the  $^1\text{H}$ - $^1\text{H}$  COSY spectrum of **2**, the cross-peaks between H<sub>2</sub>-4 with both H<sub>2</sub>-3 and H<sub>2</sub>-5 and between H-7 and H<sub>2</sub>-11, together with their chemical shifts and coupling patterns, demonstrated that there were two vicinal coupling aliphatic units in the aglycone moiety. In the HMBC spectrum of **2**, correlations from H<sub>3</sub>-13 to C-1, C-2, C-3, and C-6 and from H<sub>3</sub>-14 to C-2, C-5, C-6, and C-7 (Fig. 2)

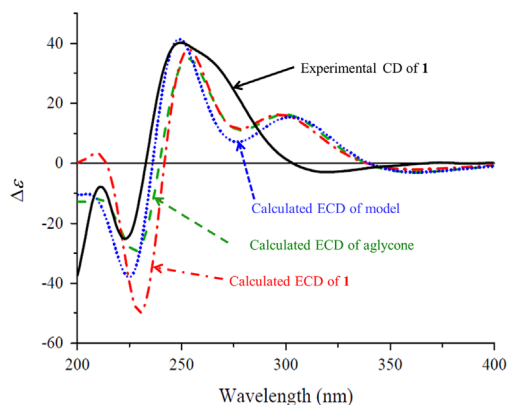


**Figure 3** The experimental CD spectrum of **1** (black) and the calculated ECD spectra of **1** (dashed red) and its aglycone (dash-dotted blue) and the model compound (dotted green) in MeOH.

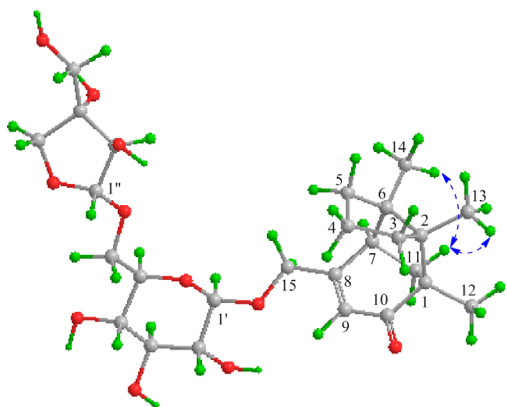


**Figure 4** The NOE enhancements induced by irradiation of H-11a (dashed arrows) for compound **2**.

established connections between the quaternary C-2 with C-1, C-3, C-6, and C-13 and between the quaternary C-6 with C-2, C-5, C-7, and C-14. These connections formed a 2,6-disubstituted 2,6-dimethyl five-membered ring. The HMBC correlations from H<sub>3</sub>-12 to C-1, C-2, C-10, and C-11 revealed linkages between the quaternary C-1 with C-10, C-11, and C-12, and confirmed the connection between the two quaternary carbons C-1 and C-2. The linkages built up a 1-methyl five-membered ring fused with the former. In addition, the HMBC correlations from H-7 to C-8, C-9, and C-15; from H-9 to C-1, C-7, and C-15; from H<sub>2</sub>-15 to C-8 and C-9; together with the chemical shifts of these proton and carbon resonances, demonstrated that both the oxymethylene (C-15) and the methine (C-7) were connected to one end (C-8) of the trisubstituted double bond and that the quaternary C-1 was linked *via* the carbonyl (C-10) to the other end (C-9). This constructed an 8-oxymethylene cyclohexene ring fused with the latter five-membered ring to give the tricyclic bridged structure of the aglycone in **2**. The presence of  $\beta$ -apiofuranosyl-(1'' $\rightarrow$ 6')- $\beta$ -glucopyranosyl was confirmed by the <sup>1</sup>H-<sup>1</sup>H COSY and HMBC correlations similar to those of **1**. Meanwhile, the HMBC correlations from H<sub>2</sub>-15 to C-1' and from H-1' to C-15 verified that the diglycosyl is located at C-15 of the aglycone. In the NOE difference spectrum of **2**, irradiation of H-11 enhanced H<sub>3</sub>-13 and H<sub>3</sub>-14 (Fig. 4), indicating that the bridge methylene (CH<sub>2</sub>-11) and the two methyl groups were oriented in the same direction. Using the same protocol as described for **1**, the *D*-configuration was

assigned for the two glycosyl units in **2**. The CD spectrum of **2** displayed a negative Cotton effect at 330 nm ( $\Delta\epsilon -2.32$ ) for the  $n \rightarrow \pi^*$  transition of cyclohexanone chromophore. Based on the octant rule for cyclohexenones<sup>22,23</sup>, the Cotton effect suggested that **2** possesses 1*S*,7*R* configuration (Fig. 5), which was further supported by comparison of the experimental CD spectrum of **2** with the calculated ECD spectra of **2** and the aglycone methyl ether (model compound) (Fig. 6). Thus, the structure of compound **2** was determined and named codonopsesquioside B, which is the first glycoside of gymnomitrane-sesquiterpenoids. According to nomenclature of the parent skeleton of gymnomitrol<sup>24</sup>, this compound is systematically named (-)-(1*S*,2*R*,6*R*,7*R*)-1,2,6-trimethyl-8-hydroxy methyltricyclic[5.3.1.0<sup>2,6</sup>]-undec-8-en-10-one  $\beta$ -*D*-apiofuranosyl-(1'' $\rightarrow$ 6')- $\beta$ -*D*-glucopyranoside.

Compound **3** was obtained as a white amorphous powder with  $[\alpha]_D^{20} +94.2$  (*c* 0.15, MeOH). Its molecular formula C<sub>21</sub>H<sub>30</sub>O<sub>8</sub> was determined by HR-ESI-MS at *m/z* 433.1827 [M+Na]<sup>+</sup> (Calcd. for C<sub>21</sub>H<sub>30</sub>O<sub>8</sub>Na, 433.1833) combined with the NMR data (Table 1). The NMR spectra of **3** resembled those of atractylenolide III that was previously reported from the same plant *C. pilosula*<sup>25,26</sup> and also obtained in this study, except for the presence of signals due to an additional  $\beta$ -glucopyranosyl unit. This suggests that **3** is the  $\beta$ -glucopyranoside of atractylenolide III, which was proved by experiments of 2D NMR and enzymatic hydrolysis. Especially, in the HMBC spectrum of **3**, the correlation from H-1' to C-8 (Fig. 2) confirmed that the  $\beta$ -glucopyranosyloxy was located at C-8. In addition, from the hydrolysate of **3** with snailase, *D*-glucose and atractylenolide III were isolated and identified by comparison of their NMR spectroscopic and specific rotation data with those of the authentic samples (see in Experimental section and Supporting information). The absolute configuration of atractylenolide III was supported by comparison of the experimental CD and calculated ECD spectra (Fig. 7). Therefore, the compound **3** was determined and named codonopsesquioside C. This compound can also be named atractylenolide III  $\beta$ -*D*-glucopyranoside based on the known aglycone.

Comparison of the experimental CD spectra with the ECD spectra predicted from TDDFT calculations has become a recent approach increasingly applied for the determination of absolute configurations of natural products<sup>20</sup>, and some flexible units including the glycosyls were occasionally replaced<sup>27</sup>. Since we previously noted that the calculated ECD spectra of several bisindole glucosides were significantly disturbed by the chiral glucopyranosyloxy group on the indole chromophores<sup>14</sup>, to further investigate the influence of the glycosyl moieties on the ECD calculations of natural products with different chromophores and support the absolute configuration assignments, the ECD spectra of **1**–**3** and their aglycones, as well as the model compounds with substitution of the diglycosyl unit in **1** and **2** by a methyl group, were calculated. As shown in Fig 3, the ECD spectra of **1**, its aglycone, and the model compound displayed Cotton effects with different intensities at similar wavelengths, indicating that the Cotton effect intensities, especially those at the shorter wavelengths, were disturbed by the substituents at C-11. As compared to those in the experimental CD spectra of **1** and the reported analogues<sup>19,28</sup>, the similar split Cotton effects between 210 and 270 nm, arising from coupling between the  $\pi \rightarrow \pi^*$  transitions of the cyclohexanone and conjugated dienol chromophores, were observed in the calculated ECD spectra, whereas the Cotton effect around 300 nm for the  $n \rightarrow \pi^*$  transition of cyclohexanone chromophore has not only different intensities but also opposite signs. Because the exciton chirality method was proved to be applicable



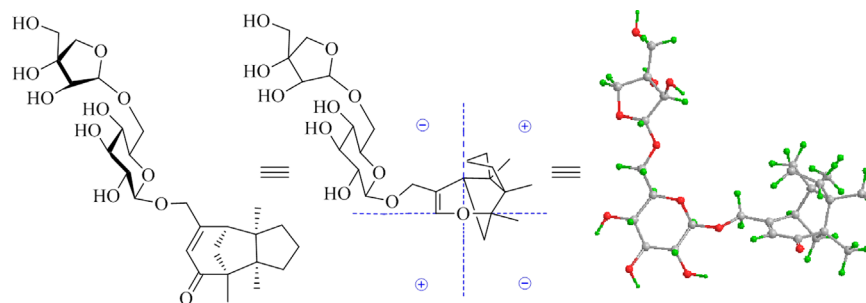


**Figure 5** The octant projection and relationship between chirality and sign of the  $n \rightarrow \pi^*$  transition Cotton effect of compound **2**.

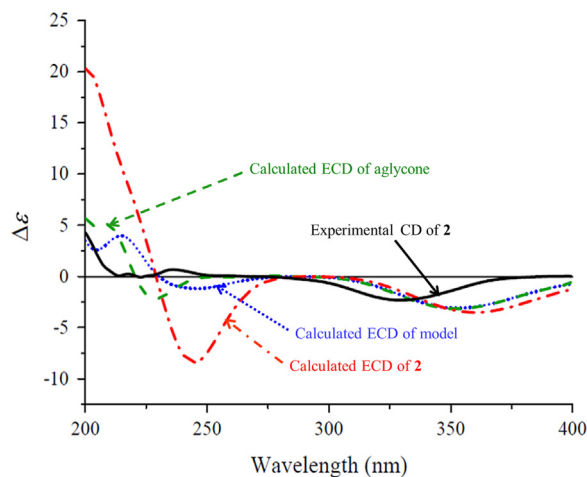


**Figure 6** The experimental CD spectrum of **2** (black) and the calculated ECD spectra of **2** (dashed red) and its aglycone (dash-dotted blue) and the model compound (dotted green) in MeOH.

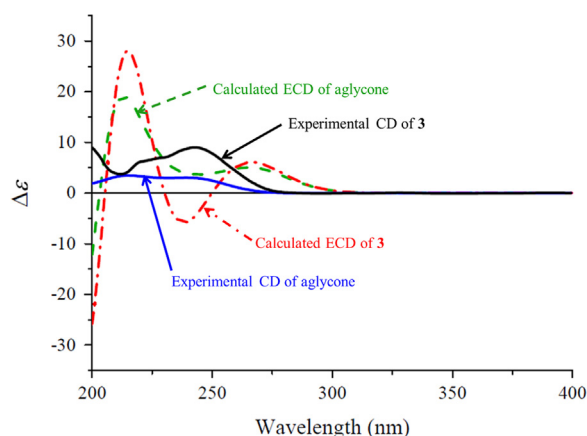


**Figure 7** The experimental CD (black and red) and calculated ECD spectra (dashed red and green) of **3** and its aglycone in MeOH.

for determination of the absolute configurations of the related analogues<sup>28</sup>, the configuration of **1** was supported by similarity of the split Cotton effects between the experimental CD spectrum of **1** and the calculated ECD spectra. In addition, because the Cotton effects around 300 nm had the opposite signs in the experimental CD and calculated ECD spectra, the empirical octant rule for the measured  $n \rightarrow \pi^*$  transition Cotton effect of cyclohexenones<sup>22,23</sup> is invalid for **1** and the reported analogues<sup>19,28</sup>.

The ECD spectra of **2**, its aglycone, and the model compound (Fig. 6) exhibited almost overlapping Cotton effects for the  $n \rightarrow \pi^*$

transition of cyclohexanone chromophore, while the intensities and wavelengths for the  $\pi \rightarrow \pi^*$  transition Cotton effects were affected by the substituents at C-15. In the experimental spectrum of **2** and the calculated ECD spectra, the sign and intensity of the  $n \rightarrow \pi^*$  transition Cotton effects were consistent with each other though the wavelengths of the calculated Cotton effects were red-shifted around 20 nm. This argues that the empirical octant rule for the experimental  $n \rightarrow \pi^*$  transition of cyclohexenones<sup>22,23</sup> is valid for **2** and its analogues (Fig. 5). In addition, the calculated ECD spectra of **3** and its aglycone showed completely different curves (Fig. 7), revealing the significant influence on the Cotton effects by the glucopyranosyl group. In this case, application of the empirical CD rules for the  $\pi \rightarrow \pi^*$  and  $n \rightarrow \pi^*$  transitions of  $\alpha, \beta$ -unsaturated  $\gamma$ -lactones<sup>29</sup> failed to predict the configurations of **3** and the aglycone. Because the calculated ECD and measured CD curves were completely different, direct comparison of the calculated and experimental spectra of **3** also failed to assign the configuration. However, similarity of curve shapes between the calculated and experimental spectra of the aglycone provided a support for the configuration assignment.

Together with our previous work<sup>14</sup>, the ECD calculations carried out in this study indicate that the glycosyl moieties have a variety of influences on the intensities, wavelengths, and signs of the Cotton effects from both the  $\pi \rightarrow \pi^*$  and  $n \rightarrow \pi^*$  transitions of the different chromophores. In the ECD calculations, replacement of the glycosyl units may result in an ambiguous assignment of the absolute configurations<sup>14</sup>. The direct comparison of the calculated and experimental spectra of glycosides may also lead to an inconclusive result<sup>27</sup>, such as **3**. To unambiguously assign the absolute configurations of the glycosides, ECD spectral calculations of both the glycoside and aglycone should be carried out and compared with the corresponding experimental CD spectra. Moreover, ECD calculations may validate whether the empirical CD rules<sup>22,23,29</sup> are valuable to predict the configurations. The empirical CD rules for the  $\pi \rightarrow \pi^*$  and/or  $n \rightarrow \pi^*$  transitions of the specific chromophores may be applicable only when the measured and calculated Cotton effects are consistent with each other.

A literature survey demonstrates that compound **1** is the first diglycoside of C<sub>15</sub> carotenoid sesquiterpenoids mainly consisting of abscisic acid (ABA) derivatives<sup>19</sup>. Among the C<sub>15</sub> carotenoids, ABA is a widely investigated phytohormone with multiple functions regulating numerous physiological processes in plant growth and development<sup>30</sup> and ingested by humans on a daily basis to mediate many beneficial health effects<sup>31</sup>. ABA is also endogenously produced and released from monocytes, granulocytes, microglia, and insulin-secreting cells with local actions and enhances the ability of pancreatic  $\beta$ -cells to secrete insulin<sup>32–34</sup>. Pharmacological studies demonstrated that ABA is involved in various immune and inflammatory responses and has potential in animal models to treat diabetes,

atherosclerosis, and inflammatory bowel disease<sup>31</sup>. Recently, it was found that ABA is a blocker of the bitter taste G protein-coupled receptor T2R4<sup>35</sup>. Therefore, characterization of compound **1** adds a new form to the ABA derivatives with diverse biological functions for future in-depth investigation.

All the reported gymnomitrane-type sesquiterpenes were isolated from lower polar essential oils or extracts of liverworts with chemotaxonomic importance<sup>24,36–41</sup>, except for three derivatives from fungal cultures<sup>42,43</sup> and fruiting bodies<sup>44</sup> and only one from a higher plant<sup>45</sup>. Compound **2** represents the first glycosidic gymnomitrane sesquiterpene. However, there are several unresolved issues with this type of sesquiterpenes in the literature. The first problem is the configuration of bridge-head atoms. To date, all the references indicate that the skeletal configuration of gymnomitrane sesquiterpenes from the liverworts is conservative. (+)-Isogymnomitrene and (–)-gymnomitrene, (+)- $\alpha$ - and (–)- $\beta$ -barbatenes, and (+)- $\alpha$ - and (–)- $\beta$ -pompenes are three pairs of synonymous compounds, of which the structures were independently determined. The skeletal configuration of gymnomitrane sesquiterpenes was assigned on the basis of the CD data of gymnomitrol-derived analogues<sup>24,36,37</sup>. X-ray crystallographic analysis of (+)- $\alpha$ -pompene- and (–)-gymnomitrene-derived *p*-bromobenzoates<sup>39,41</sup> not only verified the absolute configuration assignment, but also confirmed that (+)- $\alpha$ - and (–)- $\beta$ -pompenes are identical to (+)-isogymnomitrene and (–)-gymnomitrene, respectively, as well as to (+)- $\alpha$ - and (–)- $\beta$ -barbatenes. Unfortunately, the orientation of the bridge-unit (methylene, oxymethine, or ketone) in the structural drawings was ignored in most of the references<sup>40,41,43,45,46,48,49,51,52,54,55</sup>, which causes incorrect illustration of the configurations at the bridge-head atoms. Even in the literature reporting X-ray diffraction analysis<sup>41</sup>, the orientation of the bridge-methylene and bridge-head H and Me are not properly illustrated in the structural drawing of the reported analogues, wherein the orientation of bridge-methylene is inconsistent with that in a perspective view of the crystal molecular structure. Thus, the absolute configuration of bridge-head atoms, as determined by X-ray crystallographic analysis, should clearly and correctly be illustrated in the structure drawing of gymnomitrane sesquiterpenes.

Secondly, many numbering patterns of the skeletal atoms exist in the literature, *e.g.* (1) starting at the quaternary bridge-head atom then the neighboring quaternary angular atom and the others: without numbering of the substituent groups (methyl/hydroxymethylene/exomethylene)<sup>24</sup> and with the substituent groups numbered 13, 14, 15, and 12<sup>46–48</sup>, (2) starting at the bridge-head methine then the neighboring quaternary angular atom and the others: with the substituent groups numbered 14, 13, 12, and 15<sup>42,44</sup>; and (3) starting at the bridge-methylene followed by the bridge-head methine then the  $sp^2$  hybrid carbon and the others: with the substituting groups correspondingly numbered 13, 14, 15, and 12<sup>41</sup> and 14, 13, 12, and 15<sup>43,49–55</sup>. These descriptions have resulted in severe nomenclature confusions of the reported compounds based on the parent structure of gymnomitrane. Therefore, according to the systematic nomenclature of gymnomitrol<sup>24</sup>, the numbering and structure illustrated by **2** (Fig 1) is recommended, wherein the substituent group at the lower numbered skeletal atom is given the lower number and the bridge-unit has the same orientation as that of the angular methyl groups.

Additionally, among the three gymnomitrane sesquiterpenes from the fungi<sup>42–44</sup>, X-ray crystallographic analysis of antrodin F<sup>43</sup> demonstrated that this compound has the same skeletal configuration as that from the liverworts. For the only gymnomitrane analogue reported from a higher plant, (–)- $\alpha$ -barbatenal<sup>45</sup>, because its  $\text{LiAlH}_4$  reduction product  $[\alpha]_{\text{D}}^{20} -87$  (*c* 0.08)

showed an opposite Cotton effect at  $\lambda_{201\text{ nm}}$  to that of the (+)- $\alpha$ -barbatene<sup>37</sup>, the configuration of (–)- $\alpha$ -barbatenal was determined to be reversed to the latter. Identity of the reported NMR data of (–)- $\alpha$ -barbatenal-reduction product<sup>45</sup> and gymnomitr-3-en-12-ol {3-gymnomitren-15-ol from the liverwort,  $[\alpha]_{\text{D}}^{20} +27$  (*c* 0.17)}<sup>50</sup> confirmed that these two compounds had the same planar structure. The  $[\alpha]_{\text{D}}^{20}$  values for the two compounds were opposite, there was a large gap between the amplitudes. This prompted us to calculate the ECD spectrum of (–)- $\alpha$ -barbatenal-reduction product (see in Supporting information). For the reported configuration<sup>45</sup>, the calculated ECD spectrum exhibited the Cotton effect at 201 ( $\Delta\epsilon -1.60$ ) nm, which is consistent with the reported data and supported the configuration assignment of (–)- $\alpha$ -barbatenal. This, together with the structure determination of **2**, demonstrates that the skeletal configuration of gymnomitranes from higher plants is indeed reversed to that from the liverworts and fungi.

### 3. Conclusions

Three new metabolite codonopsesquilosides A–C (**1–3**), belonging to C<sub>15</sub> carotenoid-, gymnomitrane-, and eudesmane-types of sesquiterpenoids, respectively, were isolated from the aqueous extract of *C. pilosula* roots. Compounds **1** and **2** represent unique diglycosides of the C<sub>15</sub> carotenoids and gymnomitrane-sesquiterpenes. The ECD calculations of **1–3**, their aglycones, and the model compounds showed that the glycosyl moieties have a variety of influences on the intensities, wavelengths, and signs of the Cotton effects from both the  $n \rightarrow \pi^*$  and  $n \rightarrow \pi^*$  transitions of different chromophores. To unambiguously assign the absolute configurations, the ECD spectra of the glycoside and aglycone should be calculated and compared with the corresponding experimental CD spectra. All the reported gymnomitrane derivatives from liverworts and fungi have the same skeletal configuration, whereas those from the higher plant have a reversed configuration. To avoid confusion in the nomenclature and illustrating configurations, the numbering of skeletal atoms and the orientation of bridge-unit as shown for **2** (Fig 1) are recommended for gymnomitrane-sesquiterpenoids. Although the biological activity of **1–3** was not assayed in this study due to limited amounts of these samples, the results provide guidance for future studies of the synthesis, chemical transformation, structural modification, biosynthesis, and biological evaluation of these diverse sesquiterpenoids, as well as their potential contribution to the traditional uses of the *C. pilosula*.

### 4. Experimental

#### 4.1. General experimental procedures

Optical rotations were measured on P-2000 polarimeter (JASCO, Tokyo, Japan). UV spectra were measured on a V-650 spectrometer (JASCO, Tokyo, Japan). IR spectra were recorded on a Nicolet 5700 FT-IR microscope instrument (FT-IR microscope transmission) (Thermo Electron Corporation, Madison, USA). NMR spectra were obtained at 500 MHz or 600 MHz for <sup>1</sup>H NMR, and 125 MHz or 150 MHz for <sup>13</sup>C NMR, respectively, on Inova 500 or SYS 600 (Varian Associates Inc., Palo Alto, USA) or Bruker 600 NMR spectrometers (Bruker Corp., Switzerland) in MeOH-*d*<sub>4</sub> with solvent peak used as references. ESI-MS and

HR-ESI-MS data were measured using an AccuToFCS JMS-T100CS spectrometer (Agilent Technologies, Ltd., Santa Clara, USA). Column chromatography (CC) was performed with HPD-110 (Cangzhou Bon Absorber Technology Co. Ltd., Cangzhou, China), MCI gel CHP 20P (Mitsubishi Chemical Inc., Tokyo, Japan), silica gel (200–300 mesh, Qingdao Marine Chemical Inc., Qingdao, China), Sephadex LH-20 (Pharmacia Biotech AB, Uppsala, Sweden), or Toyopearl HW-40F (Tosoh Corporation, Tokyo, Japan). HPLC separation was performed on an instrument consisting of an Agilent ChemStation for LC system, an Agilent 1200 pump, and an Agilent 1100 single-wavelength absorbance detector (Agilent Technologies, Ltd.) with a YMC-Pack Ph column (250 mm × 10 mm, i.d.) packed with phenyl-silica gels (5 μm) (YMC Co. Ltd., Kyoto, Japan) or a Grace column (250 mm × 10 mm, i.d.) packed with C18 reversed phase silica gel (5 μm) (W.R. Grace & Co., Maryland, USA). TLC was carried out with precoated silica gel GF<sub>254</sub> glass plates (Qingdao Marine Chemical Inc., China). Spots were visualized under UV light or by spraying with 7% H<sub>2</sub>SO<sub>4</sub> in 95% EtOH followed by heating. Unless otherwise noted, all chemicals were obtained from commercially available sources and were used without further purification.

#### 4.2. Plant material

The roots of *C. pilosula* were collected in October 2012 from a culture field in Weiyuan, Gansu Province, China. Plant identity was verified by Mr. Lin Ma (Institute of Materia Medica, Beijing, China). A voucher specimen (No. ID-S-2503) was deposited at the herbarium of the Department of Medicinal Plants, Institute of Materia Medica, Beijing, China.

#### 4.3. Extraction and isolation

The dried and powdered roots of *C. pilosula* (50 kg) were decocted with H<sub>2</sub>O (150 L, 3 × 0.5 h). The decoction was evaporated under reduced pressure to yield a brown residue (26 kg). The residue was dissolved in H<sub>2</sub>O (100 L), loaded on a macroporous adsorbent resin (HPD-110, 20 L) column (200 cm × 20 cm), and eluted successively with H<sub>2</sub>O (100 L), 50% EtOH (120 L), and 95% EtOH (80 L) to yield three corresponding fractions A–C. Fraction B (270 g) was chromatographed over MCI gel CHP 20 P (5.5 L), successively eluting with H<sub>2</sub>O (20 L), 30% EtOH (30 L), 50% EtOH (30 L), and 95% EtOH (8 L), to give B1–B4. Fraction B3 (22 g) was subjected to flash chromatography over reverse phase (RP) silica gel, eluting with a gradient of increasing MeOH (40–100%) in H<sub>2</sub>O, to yield subfractions B3-1–B3-5. B3-1 (10 g) was fractionated by CC over silica gel, eluting with a gradient of increasing MeOH (0–100%) in CHCl<sub>3</sub>, to yield B3-1-1–B3-1-10, of which B3-1-9 (1.1 g) was further separated by CC over HW-40 F using MeOH as the mobile phase to give B3-1-9-1–B3-1-9-5. Purification of B3-1-9-1-2 (80 mg) by RP-HPLC (C18 column, 1.5 mL/min, UV 220 nm) with CH<sub>3</sub>OH–H<sub>2</sub>O (58:42, v/v) as the mobile phase yielded **1** (1.6 mg, *t*<sub>R</sub> = 34 min). Fractionation of B3-2 (5.3 g) by CC over silica gel, eluting with a gradient of increasing MeOH (0–100%) in CHCl<sub>3</sub>, yielded B3-2-1–B3-2-6, of which B3-2-1 (1.0 g) was further fractionated by CC over Sephadex LH-20 (CHCl<sub>3</sub>–MeOH, 1:1, v/v) to give B3-2-1-1–B3-2-1-8. Purification of B3-2-1-3 (100 mg) by RP-HPLC (Ph column, 1.5 mL/min, UV 220 nm) with CH<sub>3</sub>OH–H<sub>2</sub>O (60:40, v/v) as the mobile phase yielded **2** (3.0 mg, *t*<sub>R</sub> = 37 min). B3-4

(2.5 g) was separated by CC over silica gel, eluting with a gradient of increasing MeOH (0–100%) in CHCl<sub>3</sub>, to afford B3-4-1–B3-4-10. Subsequent isolation of B3-4-4 (150 mg) by RP-HPLC (C18 column, 1.5 mL/min, UV 280 nm) with CH<sub>3</sub>OH–H<sub>2</sub>O (66:34, v/v) as the mobile phase obtained **3** (8.0 mg, *t*<sub>R</sub> = 28 min).

##### 4.3.1. Codonopsesquiloside A (**1**)

White amorphous powder;  $[\alpha]_{\text{D}}^{20} +26.3$  (*c* 0.04, MeOH); UV (MeOH)  $\lambda_{\text{max}}$  (log $\epsilon$ ) 237 (5.69), 344 (4.74) nm; CD (MeOH) 223 ( $\Delta\epsilon -25.15$ ), 250 ( $\Delta\epsilon +40.24$ ), 320 ( $\Delta\epsilon -2.88$ ) nm; IR  $\nu_{\text{max}}$  3395, 3189, 3010, 2921, 2849, 1646, 1468, 1419, 1373, 1324, 1301, 1246, 1215, 1118, 1053, 1018, 817, 721, 646 cm<sup>-1</sup>; <sup>1</sup>H NMR (DMSO-*d*<sub>6</sub>, 600 MHz) data, see Table 1; <sup>13</sup>C NMR (DMSO-*d*<sub>6</sub>, 150 MHz) data, see Table 1; ESI-MS *m/z* 551 [M+Na]<sup>+</sup>, 567 [M+K]<sup>+</sup>, 563 [M+Cl]<sup>-</sup>; HR-ESI-MS *m/z* 551.2461 [M+Na]<sup>+</sup> (Calcd. for C<sub>26</sub>H<sub>40</sub>O<sub>11</sub>Na, 551.2463).

##### 4.3.2. Codonopsesquiloside B (**2**)

White amorphous powder;  $[\alpha]_{\text{D}}^{20} -46.7$  (*c* 0.04, MeOH); UV (MeOH)  $\lambda_{\text{max}}$  (log $\epsilon$ ) 203 (4.70), 239 (4.53) nm; CD (MeOH) 236 ( $\Delta\epsilon +0.66$ ), 330 ( $\Delta\epsilon -2.32$ ) nm; IR  $\nu_{\text{max}}$  3395, 3187, 3010, 2922, 2850, 1747, 1467, 1468, 1420, 1373, 1324, 1300, 1243, 1163, 1118, 1051, 914, 817, 722, 648, 548 cm<sup>-1</sup>; <sup>1</sup>H NMR (CD<sub>3</sub>OD, 600 MHz) data, see Table 1; <sup>13</sup>C NMR (CD<sub>3</sub>OD, 150 MHz) data, see Table 1; ESI-MS *m/z* 551 [M+Na]<sup>+</sup>, 567 [M+K]<sup>+</sup>, 527 [M–H]<sup>-</sup>, 563 [M+Cl]<sup>-</sup>; HR-ESI-MS *m/z* 529.2637 [M+H]<sup>+</sup> (Calcd. for C<sub>26</sub>H<sub>41</sub>O<sub>11</sub>, 529.2643), 551.2462 [M+Na]<sup>+</sup> (Calcd. for C<sub>26</sub>H<sub>40</sub>O<sub>11</sub>Na, 551.2463).

##### 4.3.3. Codonopsesquiloside C (**3**)

White amorphous powder;  $[\alpha]_{\text{D}}^{20} +94.2$  (*c* 0.15, MeOH); UV (MeOH)  $\lambda_{\text{max}}$  (log $\epsilon$ ) 203 (4.67), 222 (4.21) nm; CD (MeOH) 243 ( $\Delta\epsilon +9.01$ ) nm; IR  $\nu_{\text{max}}$  3395, 3082, 2930, 2847, 1756, 1688, 1649, 1441, 1411, 1388, 1337, 1322, 1288, 1264, 1251, 1234, 1183, 1160, 1078, 1050, 997, 950, 891, 869, 846, 768, 732, 690, 621, 572, 556 cm<sup>-1</sup>; <sup>1</sup>H NMR (acetone-*d*<sub>6</sub>, 600 MHz) data, see Table 1; <sup>13</sup>C NMR (acetone-*d*<sub>6</sub>, 150 MHz) data, see Table 1; ESI-MS *m/z* 433 [M+Na]<sup>+</sup>, 449 [M+K]<sup>+</sup>, 445 [M+Cl]<sup>-</sup>; HR-ESI-MS *m/z* 433.1827 [M+Na]<sup>+</sup> (Calcd. for C<sub>21</sub>H<sub>30</sub>O<sub>8</sub>Na, 433.1833).

#### 4.4. Enzymatic hydrolysis of **1–3** and identification of sugars in the hydrolysates

Compounds **1–3** (1.6–3.0 mg) were separately hydrolyzed in H<sub>2</sub>O (3 mL) with snailase at 37 °C for 24 h, after which the reaction mixture was extracted with EtOAc (3 × 3 mL). The EtOAc phase was concentrated under reduced pressure, and purified by RP-HPLC using the C18 column (MeOH–H<sub>2</sub>O, 75:25, v/v, 220 nm, 1.5 mL/min) for the hydrolysate of **2** and the Ph column (MeOH–H<sub>2</sub>O, 73:27, v/v, 220 nm, 1.5 mL/min) for the hydrolysate of **3** to obtain the corresponding aglycones with following physical-chemical properties. The aglycone of **2** (0.60 mg, *t*<sub>R</sub> = 20 min):  $[\alpha]_{\text{D}}^{20} +20.1$  (*c* 0.04, MeOH); <sup>1</sup>H NMR (600 MHz, acetone-*d*<sub>6</sub>)  $\delta$  5.98 (s, H-9), 4.30 (m, H-15), 2.17 (d, *J* = 4.2 Hz, H-1), 2.07 (m, H-11a), 1.80 (d, *J* = 11.4 Hz, H-11b), 1.70 (ddd, *J* = 12.6, 6.0, 3.0 Hz, H-3a), 1.52 (m, H-4a), 1.45 (m, H-3b, 4b, 5a), 1.20 (s, MeO-12), 1.15 (m, H-5b), 1.01 (s, MeO-14), 1.00 (s, MeO-13); the aglycone of **3** (1.1 mg, *t*<sub>R</sub> = 23 min):  $[\alpha]_{\text{D}}^{20} +90.5$  (*c* 0.08, CHCl<sub>3</sub>); <sup>1</sup>H NMR (600 MHz, acetone-*d*<sub>6</sub>)  $\delta$  5.97 (s, OH-8), 4.85 (s, H-15a), 4.64 (s, H-15b), 2.67 (1H, dd, *J* = 13.2, 3.0 Hz, H-6 $\alpha$ ), 2.42 (1H, t, *J* = 13.2 Hz, H-6 $\beta$ ), 2.35 (1H,



brd,  $J=13.2$  Hz, H-3 $\beta$ ), 2.23 (1H, d,  $J=13.2$  Hz, H-9 $\alpha$ ), 2.01 (1H, dt,  $J=12.6, 6.0$  Hz, H-3 $\alpha$ ), 1.95 (1H, brd,  $J=12.6$  Hz, H-5), 1.75 (3H, s, H<sub>3</sub>-13), 1.63 (2H, m, H-2), 1.54 (1H, brd,  $J=13.2$  Hz, H-1 $\alpha$ ), 1.50 (1H, d,  $J=13.8$  Hz, H-9 $\beta$ ), 1.33 (1H, dt,  $J=13.8, 4.8$  Hz, H-1 $\beta$ ), 1.05 (3H, s, H<sub>3</sub>-14). The aqueous phase was dried using a stream of N<sub>2</sub>, followed by CC over silica gel eluting with CH<sub>3</sub>CN–H<sub>2</sub>O (8:1, v/v), to yield mixtures of glucose and apiose from the hydrolysates **1** and **2** and glucose from **3**. The sugar mixtures from the hydrolysates **1** and **2** exhibited two spots on TLC (CH<sub>3</sub>CN–H<sub>2</sub>O, 6:1, v/v) with the retention factors ( $R_f$ ) identical to those of authentic D-/L-glucose ( $R_f \approx 0.33$ ) and D-/L-*apiose* ( $R_f \approx 0.27$ ). The sugar mixtures from hydrolysis of **1** and **2**, as well as the authentic D- and L-glucose and D- and L-*apiose* (0.4 mg, each), were individually reacted with L-cysteine methyl ester (1.0 mg) in pyridine (1.0 mL) at 60 °C for 60 min, then arylisothiocyanate (10  $\mu$ L) was added and reacted at 60 °C for another 60 min<sup>18</sup>. The reaction mixtures were separately analyzed by HPLC [Grace C18 (5  $\mu$ m, 250 mm  $\times$  4.6 mm), CH<sub>3</sub>CN–H<sub>2</sub>O containing 0.1% phosphoric acid, 25:75, v/v, 0.8 mL/min] and monitored by a UV detector (250 nm) at room temperature. The  $t_R$  for the derivatives of authentic D-glucose, L-glucose, D-*apiose*, and L-*apiose* were measured to be 15.30 min, 14.15 min, 24.79 min, and 13.24 min, respectively. For the derivatives of the sugar mixture from the hydrolysate of **1**, HPLC analysis displayed two peaks with the  $t_R$  values of 15.43 min and 24.55 min, which were consistent with those of the derivatives of D-glucose and D-*apiose*, respectively, and two similar peaks with the  $t_R$  values of 15.37 min and 24.44 min were observed in the reaction mixture from the hydrolysate of **2** (see in Supporting information). The glucose (1.2 mg) from the hydrolysate of **3** gave retention factor ( $R_f \approx 0.33$ ; CH<sub>3</sub>CN–H<sub>2</sub>O, 6:1, v/v) on TLC,  $[\alpha]_D^{20} +42.3$  ( $c$  0.12, H<sub>2</sub>O)], and <sup>1</sup>H NMR spectral data (D<sub>2</sub>O) consistent with those of an authentic D-glucose (see in Supporting information).

#### 4.5. ECD calculation

For details, see Supporting information. Briefly, conformational analysis of **1–3**, their aglycones, and the model compounds, were performed by using the MMFF94 molecular mechanics force field *via* the MOE software package<sup>56</sup>, respectively. The lowest-energy conformers having relative energies within 2 kcal/mol were optimized at the B3LYP/6-31+G(d) level in MeOH. The energies, oscillator strengths, and rotational strengths of the first 30 electronic excitations were calculated using the TDDFT methodology at the B3LYP/6-311++G (2d, 2p) level. ECD spectra of the conformers were simulated using the Gaussian function with a half-band width of 0.28 eV, and the final ECD spectrum of each compound was simulated according to Boltzmann weighting of each conformer. All quantum computations were performed using Gaussian 09 program package<sup>57</sup>, on an IBM cluster machine located at the High Performance Computing Center of Peking Union Medical College.

#### Acknowledgments

Financial support from the National Natural Sciences Foundation of China (NNSFC; Grant Nos. 30825044 and 20932007), the Program for Changjiang Scholars and Innovative Research Team in University (PCSIRT, Grant No. IRT1007), and the National Science and Technology Project of China (Nos. 2012ZX09301002-002 and 2011ZX09307-002-01) is acknowledged.

#### Appendix A. Supporting information

Supplementary data associated with this article can be found in the online version at <http://dx.doi.org/10.1016/j.apsb.2015.09.007>.

#### References

1. Jiangsu New Medical College. *Dictionary of traditional Chinese medicine*. vol. 1. Shanghai: Shanghai Science and Technology Publishing House; 1986, p. 1837–9.
2. Jiang YP, Liu YF, Guo QL, Jiang ZB, Xu CB, Zhu CG, et al. Acetylenes and fatty acids from *Codonopsis pilosula*. *Acta Pharm Sin B* 2015;5:215–22.
3. Chen MH, Lin S, Li L, Zhu CG, Wang XL, Wang YN, et al. Enantiomers of an indole alkaloid containing unusual dihydrothiopyran and 1,2,4-thiadiazole rings from the root of *Isatis indigotica*. *Org Lett* 2012;14:5668–71.
4. Zhao F, Wang SJ, Lin S, Zhu CG, Yue ZG, Yu Y, et al. Natural and unnatural anthraquinones isolated from the ethanol extract of the roots of *Knoxia valerianoides*. *Acta Pharm Sin B* 2012;2:260–6.
5. Yu Y, Zhu CG, Wang SJ, Song WX, Yang YC, Shi JG. Homosecoiridoid alkaloids with amino acid units from the flower buds of *Lonicera japonica*. *J Nat Prod* 2013;76:2226–33.
6. Wang F, Jiang YP, Wang XL, Wang SJ, Bu PB, Lin S, et al. Aromatic glycosides from the flower buds of *Lonicera japonica*. *J Asian Nat Prod Res* 2013;15:492–501.
7. Tian Y, Guo QL, Xu WD, Zhu CG, Yang YC, Shi JG. A minor diterpenoid with a new 6/5/7/3 fused-ring skeleton from *Euphorbia micractina*. *Org Lett* 2014;16:3950–3.
8. Xu WD, Tian Y, Guo QL, Yang YC, Shi JG. Secoeuphoractin, a minor diterpenoid with a new skeleton from *Euphorbia micractina*. *Chin Chem Lett* 2014;25:1531–4.
9. Song WX, Yang YC, Shi JG. Two new  $\beta$ -hydroxy amino acid-coupled secoiridoids from the flower buds of *Lonicera japonica*: isolation, structure elucidation, semisynthesis, and biological activities. *Chin Chem Lett* 2014;25:1215–9.
10. Yu Y, Jiang ZB, Song WX, Yang YC, Li YH, Jiang JD, et al. Glucosylated caffeoylquinic acid derivatives from the flower buds of *Lonicera japonica*. *Acta Pharm Sin B* 2015;5:210–4.
11. Guo QL, Wang YN, Zhu CG, Chen MH, Jiang ZB, Chen NH, et al. 4-Hydroxybenzyl-substituted glutathione derivatives from *Gastrodia elata*. *J Asian Nat Prod Res* 2015;17:439–54.
12. Guo QL, Wang YN, Lin S, Zhu CG, Chen MH, Jiang ZB, et al. 4-Hydroxybenzyl-substituted amino acid derivatives from *Gastrodia elata*. *Acta Pharm Sin B* 2015;5:350–7.
13. Liu YF, Chen MH, Wang XL, Zhu CG, Lin S, Xu CB, et al. Antiviral enantiomers of a bisindole alkaloid with a new carbon skeleton from the roots of *Isatis indigotica*. *Chin Chem Lett* 2015;26:931–6.
14. Liu YF, Chen MH, Guo QL, Lin S, Xu CB, Jiang YP, et al. Antiviral glycosidic bisindole alkaloids from the roots of *Isatis indigotica*. *J Asian Nat Prod Res* 2015;17:689–704.
15. Jiang YP, Liu YF, Guo QL, Jiang ZB, Xu CB, Zhu CG, et al. C<sub>14</sub>-polyacetylene glycosides from *Codonopsis pilosula*. *J Asian Nat Prod Res* 2015;17:601–14.
16. Takayanagi T, Ishikawa T, Kitajima J. Sesquiterpene lactone glycosides and alkyl glycosides from the fruit of cumin. *Phytochemistry* 2003;63:479–84.
17. Tamaki A, Ide T, Otsuka H. Phenolic glycosides from the leaves of *Alangium platanifolium* var. *platanifolium*. *J Nat Prod* 2000;63:1417–9.
18. Takana T, Nakashima T, Ueda T, Tomi K, Kouno I. Facile discrimination of aldose enantiomers by reversed-phase HPLC. *Chem Pharm Bull* 2007;55:899–901.
19. Lutz A, Winterhalter P. Isolation of additional carotenoid metabolites from quince fruit (*Cydonia oblonga* Mill.). *J Agric Food Chem* 1992;40:1116–20.



20. Li XC, Ferreira D, Ding YQ. Determination of absolute configuration of natural products: theoretical calculation of electronic circular dichroism as a tool. *Curr Org Chem* 2010;**14**:1678–97.
21. Lutz A, Winterhalter P. Abscisic alcohol glucoside in quince. *Phytochemistry* 1993;**32**:57–60.
22. Snatzke G. Circular dichroismus-VIII, modifizierung der octantenregel für  $\alpha$ ,  $\beta$ -ungesättigt ketone: theorie. *Tetrahedron* 1965;**21**:413–9.
23. Snatzke G. Circular dichroismus-IX, modifizierung der octantenregel für  $\alpha$ ,  $\beta$ -ungesättigt ketone: transoide enone. *Tetrahedron* 1965;**21**:421–438.
24. Connolly JD, Harding AE, Thornton IMS. Gymnomitrol and related sesquiterpenoids from the liverwort *Gymnomitrium obtusum* (Lindb) pears (Hepaticae). A novel tricyclic skeleton. *J Chem Soc Perkin Trans I* 1974 1974:2487–93.
25. Wang ZT, Xu GJ, Hattori M, Namba T. Constituents of the roots of *Codonopsis pilosula*. *Jap J Pharm* 1988;**42**:339–42.
26. Qi HY, Wang R, Liu Y, Shi YP. Studies on the chemical constituents of *codonopsis pilosula*. *J Chin Med Mater* 2011;**34**:546–8.
27. Tatsis EC, Schaumlöffel A, Warskulat AC, Massiot G, Schneider B, Bringmann G. Nudicaulins, yellow flower pigments of *Papaver nudicaule*: revised constitution and assignment of absolute configuration. *Org Lett* 2013;**15**:156–9.
28. Koreeda M, Weiss G, Nakanishi K. Absolute configuration of natural (+)-abscisic acid. *J Am Chem Soc* 1973;**95**:239–40.
29. Uchida I, Kuriyama K. The  $\pi \rightarrow \pi^*$  circular dichroism of  $\alpha, \beta$ -unsaturated  $\gamma$ -lactones. *Tetrahedron Lett* 1974;**15**:3761–4.
30. Wasilewska A, Vlad F, Sirichandra C, Redko Y, Jammes F, Valon C, et al. An update on abscisic acid signaling in plants and more. *Mol Plant* 2008;**1**:198–217.
31. Bassaganya-Riera J, Skoneczka J, Kingston DGJ, Krishnan A, Misyak SA, et al. Mechanisms of action and medicinal applications of abscisic acid. *Curr Med Chem* 2010;**17**:467–78.
32. Bruzzone S, Moreschi I, Usai C, Guida L, Damonte G, Salis A, et al. Abscisic acid is an endogenous cytokine in human granulocytes with cyclic ADP-ribose as second messenger. *Proc Natl Acad Sci U S A* 2007;**104**:5759–64.
33. Bruzzone S, Bodrato N, Usai C, Guida L, Moreschi I, Nano R, et al. Abscisic acid is an endogenous stimulator of insulin release from human pancreatic islets with cyclic ADP ribose as second messenger. *J Biol Chem* 2008;**283**:32188–97.
34. Magnone M, Bruzzone S, Guida L, Damonte G, Millo E, Scarfi S, et al. Abscisic acid released by human monocytes activates monocytes and vascular smooth muscle cell responses involved in atherogenesis. *J Biol Chem* 2009;**284**:17808–18.
35. Pydi SP, Jaggupilli A, Nelson KM, Abrams SR, Bhullar RP, Loewen MC, et al. Abscisic acid acts as a blocker of the bitter taste G protein-coupled receptor T2R4. *Biochemistry* 2015;**54**:2622–31.
36. Connolly JD, Harding AE, Thornton IMS. Gymnomitrol, a novel tricyclic sesquiterpenoid from *gymnomitrium obtusum* (Lindb) pears (hepaticae). *J Chem Soc Chem Commun* 1972 1972:1320–1.
37. Andersen NH, Costin CR, Kramer CM, Ohta Y, Huneck S. Sesquiterpenes of *Barbilophozia* species. *Phytochemistry* 1973;**12**:2709–16.
38. Matsuo A, Maeda T, Nakayama M, Hayashi S.  $\alpha$ -Pompene a novel tricyclic sesquiterpene hydrocarbon from the liverwort. *Bazzania pompeana*. *Tetrahedron Lett* 1973;**14**:4131–4.
39. Matsuo A, Nosaki H, Nakayama M, Kushi Y, Hayashi S, Kamijo N. The revised structure for  $\alpha$ -pompene and the absolute configurations of (+)- $\alpha$ - and (-)- $\beta$ -pompene from *Bazzania pompeana*. *Tetrahedron Lett* 1975;**16**:241–4.
40. Toyota M, Nagashima F, Asakawa Y. Gymnomitran-type sesquiterpenoids from the liverwort *Plagiochila trabeculata*. *Phytochemistry* 1988;**27**:2161–4.
41. Matsuo A, Nozaki H, Yano K, Uto S, Nakayama M, Huneck S. Gymnomitran sesquiterpenoids from the liverwort *Marsupella emarginata* var. *Patens*. *Phytochemistry* 1990;**29**:1921–4.
42. Rösslein L, Tamm C, Zürcher W, Riesen A, Zehnder M. Sambucinic acid, a new metabolite of *Fusarium sambucinum*. 45th communication on verrucarins and related compounds. *Helv Chim Acta* 1988;**71**:588–95.
43. Chen ZM, Chen HP, Wang F, Li ZH, Feng T, Liu JK. New triquinane and gymnomitran sesquiterpenes from fermentation of the basidiomycete *Antrodia albocinnamomea*. *Fitoterapia* 2015;**102**:61–6.
44. Liu JQ, Wang CF, Li Y, Luo HR, Qiu MH. Isolation and bioactivity evaluation of terpenoids from the medicinal fungus *Ganoderma sinense*. *Planta Med* 2012;**78**:368–76.
45. Achenbach H, Benirschke G. Joannesialactone and other compounds from *Joannesia princeps*. *Phytochemistry* 1997;**45**:149–57.
46. Nagashima F, Ishimaru A, Asakawa Y. Sesquiterpenoids from the liverwort *Marsupella aquatica*. *Phytochemistry* 1994;**37**:777–9.
47. Toyota M, Konoshima M, Asakawa Y. Terpenoid constituents of the liverwort *Reboulia hemisphaerica*. *Phytochemistry* 1999;**52**:105–12.
48. Scher JM, Speakman JB, Zapp J, Becker H. Bioactivity guided isolation of antifungal compounds from the liverwort *Bazzania trilobata* (L.) S.F. Gray. *Phytochemistry* 2004;**65**:2583–8.
49. Nagashima F, Momosaki S, Watanabe Y, Takaoka S, Huneck S, Asakawa Y. Sesquiterpenoids from the liverworts *Bazzania trilobata* and *Porella canariensis*. *Phytochemistry* 1996;**42**:1361–6.
50. Buchanan MS, Connolly JD, Kadir AA, Rycroft DS. Sesquiterpenoids and diterpenoids from the liverwort *Jungermannia truncata*. *Phytochemistry* 1996;**42**:1641–6.
51. Warmers U, König WA. Gymnomitran-type sesquiterpenes of the liverworts *Gymnomitrium obtusum* and *Reboulia hemisphaerica*. *Phytochemistry* 1999;**52**:1501–5.
52. Warmers U, König WA. Biosynthesis of the gymnomitran-type sesquiterpenes in liverworts. *Phytochemistry* 2000;**53**:645–50.
53. Wu CL, Kao TL. A new gymnomitran-type sesquiterpenoid from the liverwort *Cylindrocolea recurvifolia*. *J Asian Nat Prod Res* 2002;**4**:281–5.
54. Nagashima F, Kondoh M, Uematsu T, Nishiyama A, Saito S, Sato M, et al. Cytotoxic and apoptosis-inducing *ent*-kauran-type diterpenoids from the Japanese liverwort *Jungermannia truncata* Nees. *Chem Pharm Bull* 2002;**50**:808–13.
55. Adio AM, König WA. Sesquiterpenoids and norsesquiterpenoids from three liverworts. *Tetrahedron: Asymmetry* 2007;**18**:1693–700.
56. Molecular Operating Environment 2008.10. Available from: (<http://www.chemcomp.com>).
57. Gaussian 09. Available from: (<http://www.gaussian.com>).